Differential regulation of telomere and centromere cohesion by the Scc3 homologues SA1 and SA2, respectively, in human cells

Silvia Canudas and Susan Smith

Molecular Pathogenesis Program and Department of Pathology, Kimmel Center for Biology and Medicine of the Skirball Institute, New York University School of Medicine, New York, NY 10016

Replicated sister chromatids are held together until mitosis by cohesin, a conserved multisubunit complex comprised of Smc1, Smc3, Scc1, and Scc3, which in vertebrate cells exists as two closely related homologues (SA1 and SA2). Here, we show that cohesin^{SA1} and cohesin^{SA2} are differentially required for telomere and centromere cohesion, respectively. Cells deficient in SA1 are unable to establish or maintain cohesion between sister telomeres after DNA replication in S phase. The same phenotype is observed upon depletion of the telomeric protein TIN2. In contrast, in SA2-depleted cells telomere cohesion is normal, but centromere cohesion is prematurely lost. We demonstrate that loss of telomere cohesion has dramatic consequences on chromosome morphology and function. In the absence of sister telomere cohesion, cells are unable to repair chromatid breaks and suffer sister telomere loss. Our studies elucidate the functional distinction between the Scc3 homologues in human cells and further reveal an essential role for sister telomere cohesion in genomic integrity.

Introduction

Telomeres are unique heterochromatic structures (Blasco, 2007) that require specialized mechanisms for replication and cohesion. Mammalian telomeres are comprised of TTAGGG repeats and shelterin, a six-subunit complex (de Lange, 2005). The shelterin subunit TRF1, along with its binding partner TIN2, function to negatively regulate telomere length by preventing access of telomerase to telomeres (van Steensel and de Lange, 1997; Kim et al., 1999; Ancelin et al., 2002). The telomeric association of TRF1 and TIN2 can be, in turn, regulated by the poly(ADP-ribose) polymerase tankyrase 1 (Smith et al., 1998). Overexpression of tankyrase 1 leads to release of TRF1 and TIN2 from telomeres and subsequent access to telomerase and telomere elongation (Smith and de Lange, 2000; Houghtaling et al., 2004).

Tankyrase 1 is also required after DNA replication for sister telomere separation before mitosis. In the absence of tankyrase 1 sister chromatids resolve normally at centromeres and arms, but remain associated at telomeres (Dynek and Smith, 2004). This persistent telomere association is observed in multiple human cancer and normal cell types, is due to protein–protein interactions, and can be rescued by depletion of TIN2 (Canudas et al., 2007; Hsiao and Smith, 2009). Thus, sister telomeres have distinct mechanisms mediating their association after DNA replication and their separation at mitosis.

Sister chromatids are held together by cohesin, a four-subunit complex (Michaelis et al., 1997; Losada et al., 1998). Three subunits (Smc1, Smc3, and Scc1) form a triangular ring-shape complex (Anderson et al., 2002; Haering et al., 2002). The fourth subunit Scc3, which is bound to Scc1, exists as two homologues in vertebrate cells, SA1 and SA2. Cohesin complexes contain either SA1 or SA2, but not both (Losada et al., 2000; Sumara et al., 2000).

Cohesin associates with DNA before replication (Losada et al., 1998; Sumara et al., 2000), but the precise mode of binding and mechanism of cohesion has not been determined. In the widely held one-ring model, cohesion is established when the replication fork passes through the cohesin ring (Haering et al., 2002; Gruber et al., 2003). In the alternative two-ring model each sister has its own ring, which then becomes paired during DNA replication (Chang et al., 2005). In support of the two-ring model, a recent study proposed a handcuff model, where two rings (each comprised of Smc1, Smc3,

Correspondence to Susan Smith: susan.smith@med.nyu.edu

The Rockefeller University Press $30.00
J. Cell Biol. Vol. 187 No. 2 165–173
www.jcb.org/cgi/doi/10.1083/jcb.200903096

and Scc1) are linked by one molecule of Scc3 (SA1 or SA2) (Zhang et al., 2008), suggesting a critical role for SA1/SA2 in holding sister chromatids together.

It is not clear why vertebrates require two forms of Scc3. Cohesin^{SA2} is severalfold more abundant than cohesin^{SA1} in human cell lines, whereas cohesin^{SA1} is the major form in *Xenopus* eggs (Losada et al., 2000; Sumara et al., 2000), raising the potential for distinct roles for these homologues. However, any functional difference remains to be determined. We showed previously that TRF1 and TIN2 were bound to cohesin^{SA1} (but not cohesin^{SA2}) via association with SA1 (Canudas et al., 2007). Moreover, depletion of SA1 rescued the persistent sister telomere cohesion in tankyrase 1–depleted cells (Canudas et al., 2007), raising the possibility that cohesin^{SA1} might have a unique role at telomeres.

Here, we show that SA1 and TIN2 are required for telomere cohesion, whereas SA2 is required for centromere cohesion, and further, that telomere cohesion plays a crucial role in chromosome structure and genomic stability.

Results and discussion

Distinct requirements for telomere and centromere cohesion

HeLaI.2.11 cells were transfected with GFP, TIN2, SA1, or SA2 siRNA for 48 h. Immunoblot analysis indicated efficient depletion of each protein (Fig. S1). Mitotic cells were isolated by shake-off and analyzed by fluorescent in situ hybridization (FISH) with a chromosome-specific subtelomere probe 16p to measure sister telomere cohesion. In control GFP siRNA mitotic cells telomeres appeared as doublets (Fig. 1 A), indicating normal resolution of cohesion. In cells treated with TIN2 siRNA, (which, in addition to depletion of TIN2, leads to degradation of TRF1 [Canudas et al., 2007 and see Fig. S1]), telomeres also resolved into doublets; however, the distance between doublets appeared much greater than that of control cells (Fig. 1 B). Depletion of SA1 also led to an increased distance between doublets (Fig. 1 C). In contrast, telomeres in SA2-depleted cells were similar to control (Fig. 1 D). We quantified these results by measuring the distance between sister telomeres (Table S1) and plotting the frequency (Fig. 1, A–D; histograms). In GFP siRNA cells the distance ranged from 0.3 to 1.8 μm. The distance was increased in TIN2-depleted cells (range: 0.7 to 10.4 μm) and in SA1-depleted cells (range: 0.7 to 6.4 μm). SA2-depleted cells appeared similar to the control with only a few telomeres showing an increased distance. Thus, depletion of TIN2 and SA1, but not SA2, leads to a dramatic increase in the distance between sister telomeres at mitosis. Similar results were obtained with a different chromosome-specific subtelomere probe, 4p (Fig. S2 A).

Cells were next subjected to FISH analysis, with a centromere-specific (cen6) chromosome probe. In GFP siRNA cells sister centromeres were tightly associated and appeared as closely opposed doublets (Fig. 1 E), indicating normal intact centromere cohesion. Measurement of the distance between sister centromeres showed a limited range of 0.2 to 1.5 μm. Similar results were obtained for cells depleted of TIN2 or SA1 (Fig. 1, F and G). In contrast, in SA2-depleted cells sister centromeres were separated (Fig. 1 H) and measurement of the distance between centromeres (range: 0.2 to 6.0 μm) showed a dramatic increase compared with control.

Graphical representation of the average distances between telomeres and centromeres (Fig. 1 M) shows that depletion of SA1 or TIN2 leads to increased distance between sister telomeres, but has no effect on centromeres. In contrast, depletion of SA2 has limited effect on telomeres, but leads to increased distance between centromeres. Together these data indicate that TIN2 and SA1 are required for telomere cohesion. We speculate that this cohesion is mediated by association between TIN2 (and TRF1) and cohesin^{SA1} (Canudas et al., 2007). TIN2 and TRF1 do not associate with cohesin^{SA2} (Canudas et al., 2007) and consistent with this, SA2 is not required for telomere cohesion. However, SA2 is uniquely required for cohesion at centromeres.

These data are consistent with our previous studies showing that siRNA depletion of SA1 (but not SA2) or TIN2 rescued the persistent sister telomere cohesion induced by tankyrase 1 siRNA depletion. Because TIN2 siRNA leads to concomitant loss of TRF1 (Canudas et al., 2007; see Fig. S1), we are unable to singly deplete TIN2 protein. We can, however, singly deplete TRF1 protein using siRNA; we showed previously that this had no effect on TIN2 protein levels and further, that it did not rescue tankyrase 1 siRNA-induced persistent telomere cohesion (Canudas et al., 2007). Consistent with these observations, we find that siRNA depletion of TRF1 does not lead to a loss in sister telomere cohesion (Fig. S2 B). Together these data suggest a central (or more dominant) role for the telomeric protein TIN2 (over TRF1) in mediating sister telomere cohesion.

Telomere cohesion is required for cohesion between chromosome arms

We next addressed the effect of loss of telomere cohesion on chromosome arms. siRNA-treated cells were subjected to FISH analysis, with an arm (20p12) chromosome probe. In GFP siRNA mitotic cells arms appeared as doublets (Fig. 1 I), indicating normal resolution of cohesion. In cells treated with TIN2 (Fig. 1 J) or SA1 (Fig. 1 K) siRNA the distance between doublets was increased, indicating loss of cohesion between sister chromatid arms. Depletion of SA2 had no effect on arm cohesion (Fig. 1 L). Plotting the average distance between sister chromatid arms alongside telomeres and centromeres (Fig. 1 M) shows that in the absence of SA2 (despite the loss in centromere cohesion) arm cohesion is normal, similar to control cells. In contrast, in TIN2- and SA1-depleted cells centromere cohesion is normal, but arm cohesion is lost. These data suggest that loss of telomere cohesion can influence arm cohesion.

This was further investigated by analyzing chromosome morphology in siRNA cells. In vertebrate cells the bulk of cohesin is removed from chromosome arms in prophase, but cohesin persists at centromeres and in small amounts along arms until its removal at the metaphase-to-anaphase transition (Losada et al., 1998; Waizenegger et al., 2000; Giménez-Abián et al., 2004). Visualization by prometaphase spread analysis typically yields "X"-shaped chromosomes with centromeres associated

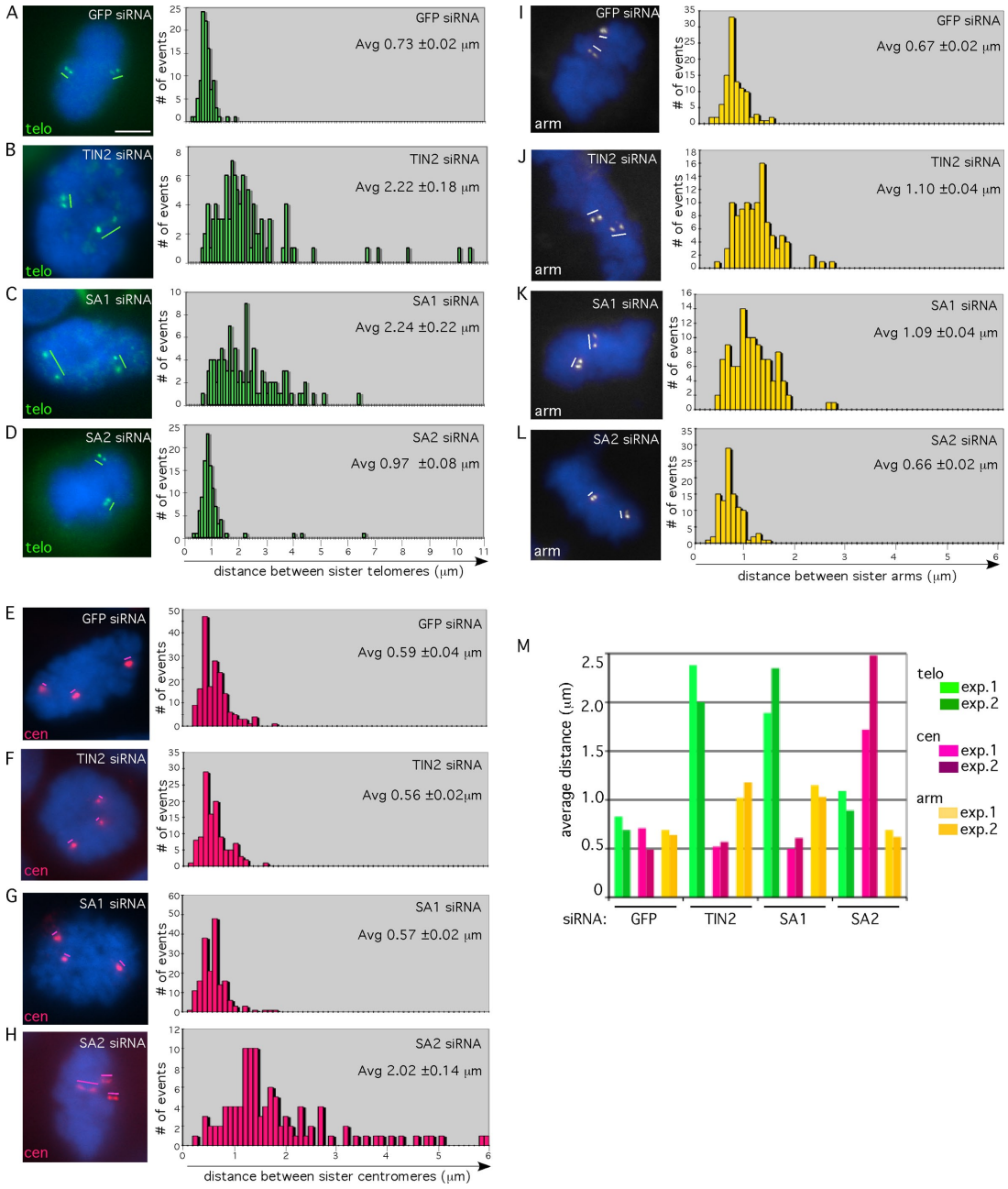

Figure 1. **TIN2 and SA1 are required for telomere and arm cohesion, whereas SA2 is required for centromere cohesion.** FISH analysis of siRNA-treated HeLa1.2.11 mitotic cells with chromosome-specific fluorescently labeled probes: (A–D) telomere 16pter (green), (E–H) centromere 6cen (red), and (I–L) arm 20p12 (white). The cen locus is trisomic. DNA was stained with DAPI (blue). Bar, 5 μm. Histograms (based on 100 measurements from two independent experiments [see Table S1]) showing the distance between FISH signals are on the right. Average (Avg) distance with SEs is indicated. (M) Graphical representation of the average distance from two independent experiments.

and arms slightly separated, as shown in the GFP siRNA control (Fig. 2 A). Depletion of TIN2 or SA1 led to an increase in the distance between telomeres/arms (Fig. 2, B and C), indicating a loss of cohesion between arms. In contrast, depletion of SA2 had only a minor effect on arms, but led to loss of centromere association (Fig. 2 D). We quantified these results by measuring the distance between sister arms (Table S2) and plotting the frequency (Fig. 2, A–D; histograms). Analysis of several hundred chromosome spreads from three independent experiments (Table I and Fig. 2 E) shows that depletion of TIN2 or SA1 (but not SA2) leads to a dramatic increase in chromosomes with separated telomeres/arms. Conversely, depletion of SA2 (but not TIN2 or SA1) leads to an increase in chromosomes lacking centromere cohesion (Fig. 2 E).

The distinct effects of SA1 and TIN2 at arms versus SA2 at centromeres are underscored by the phenotypes of the double depletions (Table S3). Depletion of both TIN2 and SA1 led to an increase in chromosomes with arms fully separated, but had no effect on centromeres (Fig. 2 F). In contrast, double depletion of SA2 with SA1 or TIN2 led to a combined phenotype, with arms fully separated and centromeres apart (Fig. 2, F and G). We note that despite the loss of cohesion at centromeres in the

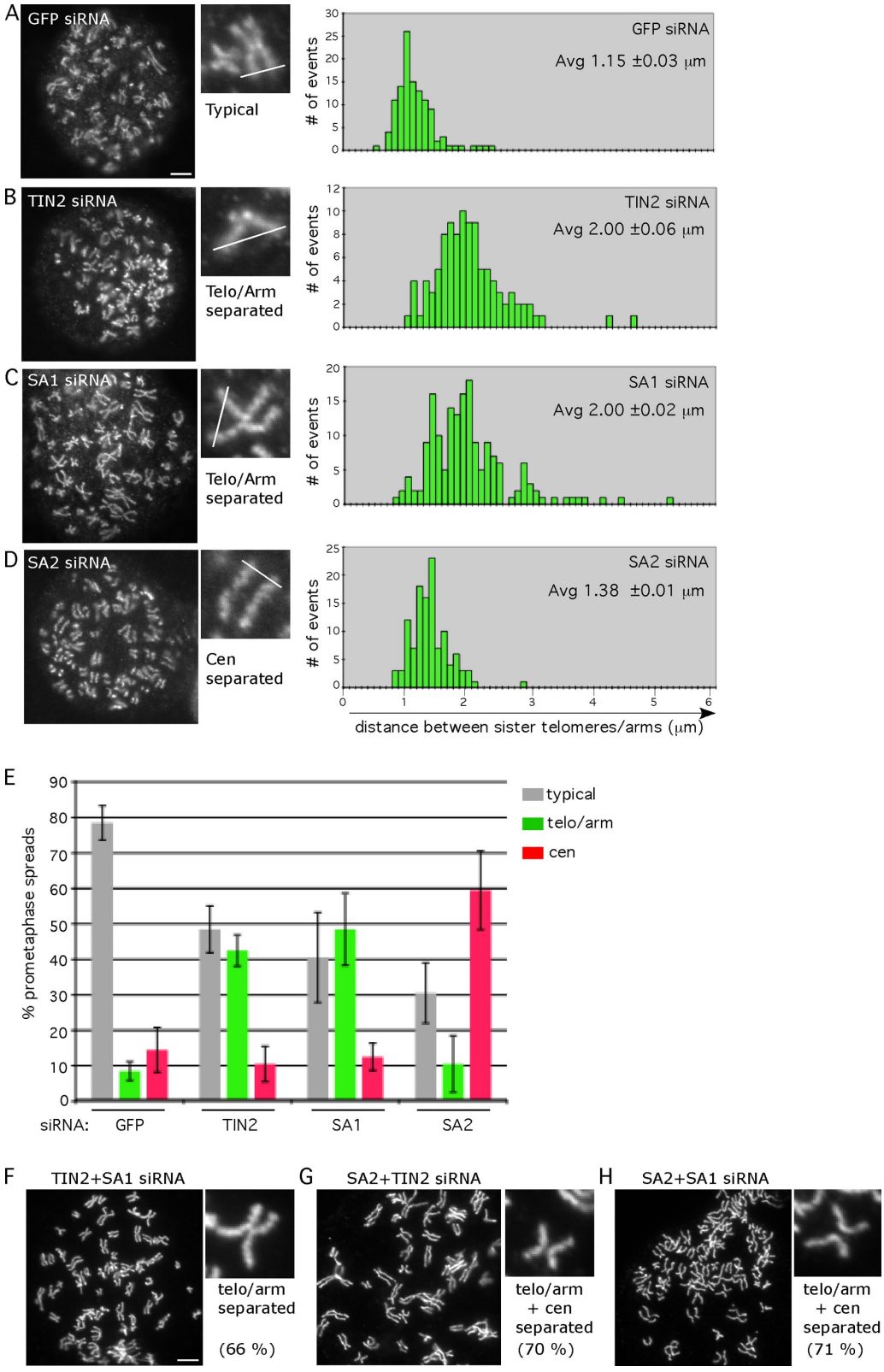

Figure 2. **SA1 and TIN2, but not SA2, are required for sister chromatid cohesion along arms.** (A–D) Chromosome spread analysis of siRNA-treated HeLaI.2.11 cells stained with antibodies to the condensin subunit Smc2. Histograms (based on ~110 measurements from three spreads [see Table S2]) showing the distance between arms are on the right. Average distance (Avg) with SEs is indicated. (E) Graphical representation of the frequency of each type of chromosome morphology. The classification was assigned when five or more chromosomes in a spread displayed the indicated morphology. Bar graphs represent the average values from three independent experiments with SDs (see Table I). (F–H) Chromosome spread analysis from double siRNA–treated cells. 150–200 spreads were scored (see Table S3). The percentage indicates the frequency of the indicated morphology. Bars, 5 μm.

Table I. **Quantification of chromosomal morphology with SDs in HeLaI.2.11 siRNA-treated prometaphase spreads**

siRNA	Spreads scored	Typical	Telomere/arm	Centromere
GFP	*n* = 66, 38, 202	51, 28, 168 (78% ± 4.8)	7, 2, 17 (8% ± 2.7)	8, 8, 17 (14% ± 6.3)
TIN2	*n* = 63, 67, 200	30, 37, 84 (48% ± 6.6)	29, 25, 85 (42% ± 4.4)	4, 5, 31 (10% ± 5.0)
SA1	*n* = 108, 112, 200	33, 38, 108 (40% ± 12.7)	57, 62, 73 (48% ± 10.2)	18, 12, 19 (12% ± 3.8)
SA2	*n* = 106, 107, 200	26, 28, 80 (30% ± 8.5)	17, 1, 26 (10% ± 8.0)	63, 74, 94 (59% ± 11.1)

absence of SA2, sister chromatids were almost always observed side by side, suggesting that SA2-depleted cells had sufficient cohesion to keep sister chromatids associated before chromosome spread preparation.

Our studies suggest that normal levels of TIN2 and SA1 are required not only for cohesion between sister telomeres, but in addition for cohesion between arms. This observation is particularly striking for TIN2, a dedicated telomeric protein. TIN2 may act to tether or immobilize cohesins at telomeres, leading to stabilization of cohesins along arms.

SA1 and TIN2 are required to establish or maintain telomere cohesion after DNA replication

To determine when during the cell cycle sister telomere cohesion was lost in TIN2- and SA1-depleted cells, we subjected cycling cells to telomere-specific FISH analysis. For detection of S phase cells, cultures were labeled with BrdU for 1 h before harvesting. The status of sister telomere cohesion was then determined by scoring doublets in BrdU-positive cells. As shown in Fig. 3, A–C, only a small fraction (16.3%) of telomeres in GFP siRNA cells showed a loss in cohesion. In contrast, cohesion was lost in 60% of telomeres in cells depleted for TIN2 or SA1. In SA2-depleted cells only a small fraction of telomeres (14%) showed a loss in cohesion (Fig. 3, A–C).

We next performed telomere FISH analysis on synchronized cells. HeLaI.2.11 cells were synchronized by double-thymidine treatment. Cells were transfected with each siRNA 4 h after release from the first thymidine arrest and processed 4 h after release from the second thymidine arrest for chromosome-specific telomere FISH (Fig. 3 D; experimental protocol). FACS analysis at 2 and 4 h after release showed that the siRNA-treated cells were progressing synchronously through S phase (Fig. S3) and at 4 h, 88–95% were in S phase (Fig 3 E). Telomere FISH analysis of the late S phase cells (Fig. 3, F and I) showed that only a small fraction of telomeres in GFP and SA2 siRNA cells lost cohesion (13 and 20%, respectively). In contrast, >60% of telomeres in TIN2- and SA1-depleted cells lost cohesion. The premature loss of cohesion in late S phase was also apparent at chromosome arms (Fig. 3, G and I); FISH analysis of TIN2- and SA1-depleted late S phase cells with an arm probe showed a fivefold increase in doublets compared with GFP cells. The premature loss of cohesion at telomeres and arms was not due to a loss in centromere cohesion; FISH analysis with a centromere probe (Fig. 3, H and I) showed no loss in centromere cohesion in TIN2- or SA1-depleted cells. In contrast, depletion of SA2 (which had only minor effects at telomeres and arms) yielded a fivefold increase in centromere doublets compared with GFP. We repeated this analysis in a second independent experiment using different probes (Fig. 3 J) and obtained similar results (shown graphically in Fig. 3 K).

Together these data show that in interphase cells TIN2 and SA1 are required for cohesion at telomeres and arms, but not at centromeres, and conversely, that SA2 is required for cohesion at centromeres, but not at telomeres and arms.

Telomere cohesion is required for DNA repair and telomere integrity

One prediction of the inability to establish or maintain telomere/arm cohesion is that it could hinder the cell's capacity to repair double-strand breaks in G2 (Sjögren and Nasmyth, 2001; Schmitz et al., 2007). To address this question, we induced double-strand breaks with 2 Gy ionizing radiation (a dose sufficient to induce double-strand breaks, but not cell cycle arrest [Tables S4 and S5]) and then analyzed the cell's ability to repair the breaks in G2 after a 2-h recovery period. When prometaphase spreads were analyzed immediately after radiation, chromatid breaks were readily detected in GFP, TIN2, SA1, and SA2 siRNA-treated cells (Fig. 4, A and B; Table II). However, when cells were analyzed after a 2-h recovery period, striking differences were observed. GFP and SA2 siRNA cells efficiently repaired chromatid breaks, whereas TIN2 and SA1 siRNA cells did not (Fig. 4 B and Table II). Because breaks occur all along sister chromatid arms, the inability to repair breaks in TIN2- and SA1-depleted cells is likely due to the loss in arm cohesion observed in these cells. We speculate that under these conditions chromatids do not have their sisters nearby and are thus unable to strand invade and repair by homologous recombination. Our experiments do not address the general role of SA1 versus SA2 in double-strand break repair. In this regard, future experiments analyzing DNA damage sensitivity in SA1- versus SA2-depleted cells should prove informative.

Finally, we asked if the failure to establish or maintain sister telomere cohesion had consequences for telomere integrity. Metaphase spreads were prepared from siRNA-treated cells and analyzed by FISH with a telomere repeat probe. As shown in Fig. 4, C and D, and Table II, we observed a dramatic increase in sister telomere loss in TIN2- or SA1-depleted cells, compared with GFP or SA2 siRNA cells. We speculate that this loss may result from the inability of sister telomeres (due to the loss in telomere cohesion) to perform homologous recombination-dependent DNA replication. This type of replication is the mainstay in ALT (alternative lengthening of telomeres) cells (Cesare and Reddel, 2008), which lack telomerase, but it may also occur at a low frequency in telomerase-positive cells. One testable prediction of this hypothesis is that depletion of SA1 or TIN2 will negatively affect telomere maintenance in ALT cells.

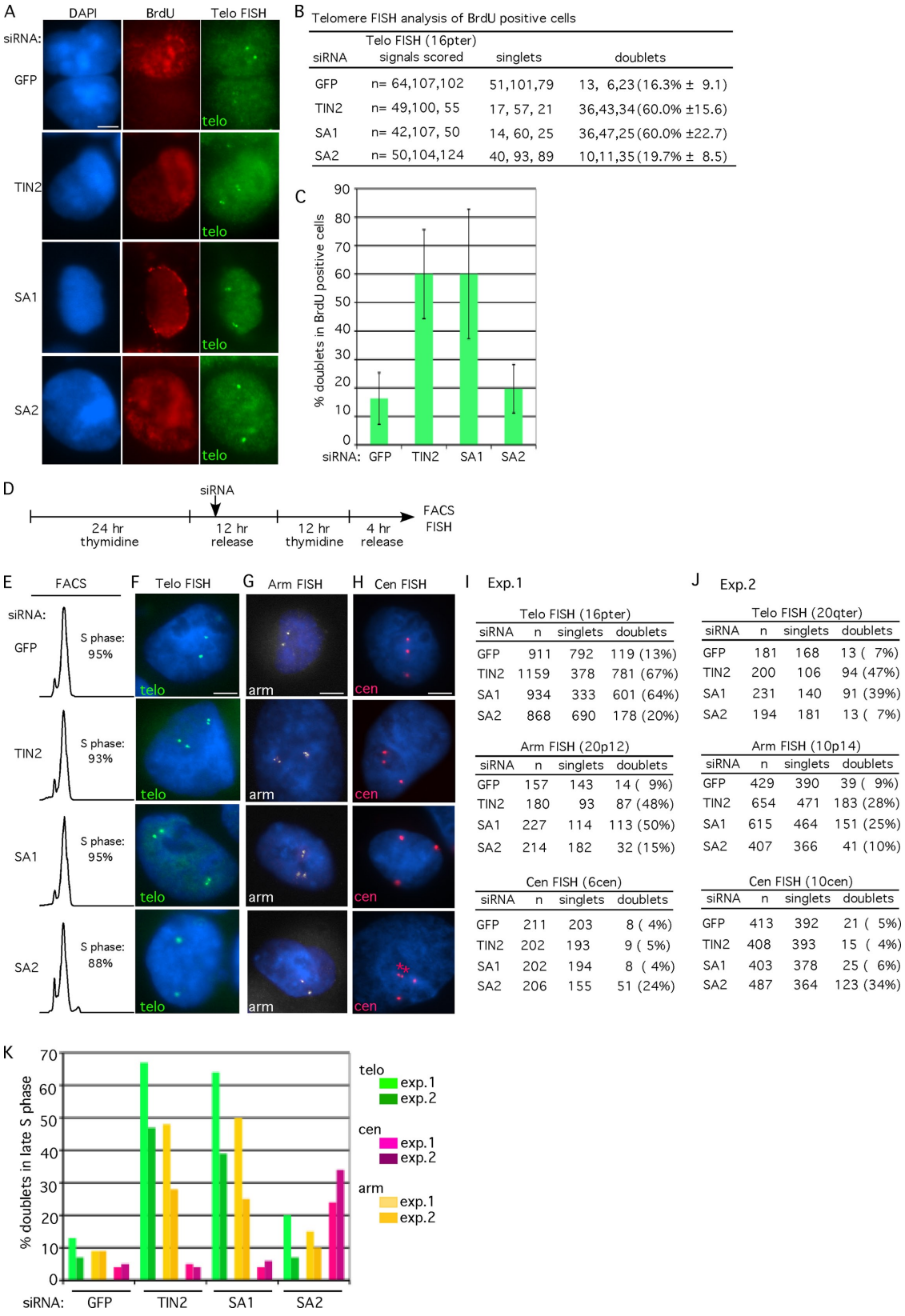

Figure 3. **Sister telomere cohesion is lost prematurely (or not established) in S phase in SA1- and TIN2-depleted cells.** (A–C) FISH analysis of BrdU-positive cells. (A) siRNA-treated HeLa1.2.11 cells were incubated with BrdU for 60 min before harvest, stained with anti-BrdU antibody (red), and hybridized with a telomere-specific fluorescently labeled probe 16pter (green). DNA was stained with DAPI (blue). (B) Table showing the number of FISH signals scored in BrdU-positive cells as singlet or doublets from three independent experiments with SDs. (C) Graphical representation of the frequency of doublets in BrdU-positive cells. Bar graphs represent the average values with SDs. (D–K) FISH analysis of late S phase synchronized cells. (D) Schematic representation of the experimental protocol to synchronize siRNA-treated cells. (E) FACS analysis and (F–H) FISH analysis of cells 4 h after release from the second thymidine

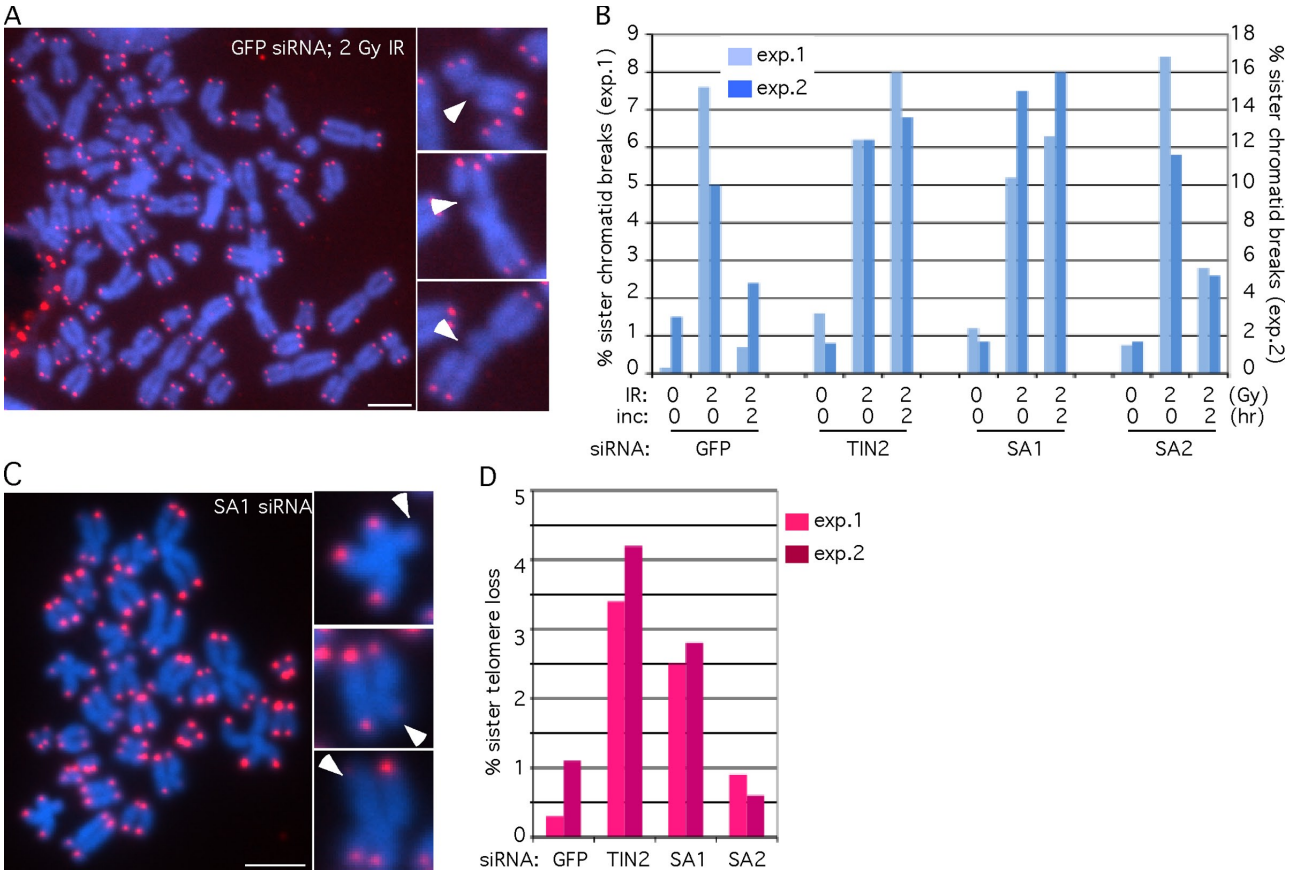

Figure 4. **Sister telomere cohesion is required for double-strand break repair and telomere maintenance.** (A and B) SA1- and TIN2-depleted cells are defective in sister chromatid repair after ionizing radiation. siRNA-treated HeLaI.2.11 cells were irradiated with 2 Gy of ionizing radiation (IR), and allowed to recover for 0 or 2 h. Prometaphase spreads were analyzed by hybridization to Cy3-conjugated telomere repeat $(CCCTAAA)_3$ peptide nucleic acid (PNA) probe (red). DNA was stained with DAPI (blue). (A) Chromosome spread of GFP siRNA cells treated with 2 Gy IR. Three enlarged examples of sister chromatid breaks (indicated by arrowheads) are shown. (B) Graphical representation of the percentage of sister chromatid breaks. Approximately 500 chromosomes were scored for each sample from two independent experiments (exp.1, x axis on the left; exp. 2, x axis on the right; see Table II). (C and D) Sister telomeres are lost in SA1- and TIN2-depleted cells. siRNA-treated HeLaI.2.11 cells were processed for PNA-FISH as described above. (C) Chromosome spread of SA1 siRNA cells. Three enlarged examples of sister telomere loss (indicated by arrowheads) are shown. Bars, 5 μm. (D) Graphical representation of the percentage of sister telomere loss. Approximately 500 chromosomes were scored for each sample from two independent experiments (see Table II).

Conclusions

Our work here reveals an essential role for telomere cohesion in chromosome structure and function. We show that TIN2 is required to establish or maintain cohesion at telomeres. We further demonstrate that a defect in telomere cohesion leads to dramatic consequences for chromosome arms, revealed by a premature loss of arm cohesion in interphase and increased separation at mitosis, and by the inability to repair sister chromatid breaks in TIN2-depleted cells. A crucial role for telomeres is highlighted by the observation that in the absence of TIN2, cohesin^{SA1} and cohesin^{SA2} together are unable to maintain telomere/arm cohesion. TIN2-mediated cohesion between sister telomeres may serve to tether or block loss of cohesin from chromosome arms.

Our studies also reveal distinct roles for SA1 versus SA2 in sister chromatid cohesion. If SA1 and SA2 were functionally the same, given that SA2 is more abundant than SA1 in HeLa cells, we would expect depletion of SA2 to have a stronger effect on cohesion than SA1. Strikingly, however, while depletion of SA2 leads to loss of centromere cohesion, it has no effect on arm or telomere cohesion. Conversely, depletion of SA1 leads to loss of arm and telomere cohesion, but has no effect at centromeres. Here, however, because SA1 is less abundant than SA2, we cannot rule out the possibility that SA1 contributes to centromere cohesion and that the more abundant SA2 is able to compensate in its absence.

Finally, we consider our data in light of the recent two-ring "handcuff" model for the cohesin complex, where each ring contains one set of Smc1, Smc3, and Scc1 molecules (and associates with one chromatid) and the two single rings are bridged by one molecule of SA1 or SA2 (Zhang et al., 2008). In

arrest. Cells were hybridized with a telomere 16pter (F, green), arm 20p12 (G, white), or centromere 6cen (H, red) probe. Asterisks indicate a centromere that has lost cohesion. DNA was stained with DAPI (blue). Bars, 5 μm. (I) Tables showing the FISH signals scored as singlets or doublets from exp. 1 for the telomere (16pter), arm (20p12), or centromere (6cen) probe. (J) Tables showing the FISH signals scored as singlets or doublets from exp. 2 for the telomere (20qter), arm (10p14), or centromere (10cen) probe. (K) Graphical representation of the frequency of doublets from two independent experiments.

Table II. **Analysis of chromosomal aberrations in HeLa1.2.11 siRNA-treated cells**

siRNA	Exp. #	Chromosomes scored	IR(Gy)	Inc.	Sister chromatid breaks	Sister telomere loss
		n		*h*		
GFP	1, 2	605, 567	0	0	1 (0.2%), 17 (3.0%)	2 (0.3%), 6 (1.1%)
	1, 2	574, 667	2	0	44 (7.6%), 67 (10.0%)	ND
	1, 2	555, 591	2	2	4 (0.7%), 28 (4.7%)	ND
TIN2	1, 2	493, 666	0	0	8 (1.6%), 11 (1.6%)	17 (3.4%), 28 (4.2%)
	1, 2	653, 644	2	0	41 (6.2%), 80 (12.4%)	ND
	1, 2	631, 540	2	2	51 (8.0%), 73 (13.5%)	ND
SA1	1, 2	487, 743	0	0	6 (1.2%), 13 (1.7%)	12 (2.5%), 21 (2.8%)
	1, 2	462, 452	2	0	24 (5.2%), 68 (15.0%)	ND
	1, 2	533, 506	2	2	34 (6.3%), 81 (16.0%)	ND
SA2	1, 2	660, 681	0	0	5 (0.8%), 12 (1.7%)	6 (0.9%), 4 (0.6%)
	1, 2	578, 632	2	0	49 (8.4%), 73 (11.5%)	ND
	1, 2	557, 643	2	2	16 (2.8%), 33 (5.1%)	ND

this model SA1 and SA2 play a central role acting as linkers to hold the rings, and hence the sister chromatids, together. Consistent with this study, we show that depletion of SA1 or SA2 leads to loss of cohesion, and further, that this can occur at distinct chromosomal domains. We speculate that distinct effects of SA1 and SA2 on cohesion at different chromosomal domains may be mediated by unique protein–protein interactions: SA1 with the telomeric proteins TIN2 and TRF1, and SA2 with (as yet to be identified) centromeric proteins.

Materials and methods

siRNA transfection
siRNA transfections were performed in HeLa1.2.11 cells, a HeLa-derived clonal cell line (van Steensel et al., 1998) with Oligofectamine (Invitrogen) for 48 h according to the manufacturer's protocol. The final concentration of siRNA was 100 nM. For double-siRNA experiments each oligo was present at 50 nM. The following siRNAs (synthesized by Thermo Fisher Scientific and described previously [Canudas et al., 2007]) were used: TIN2.a (5′-AACGCCUUUGUAUGGGCCUAA-3′); SA1.a (5′-GUGAUGCCUUCCUAAAUGA-3′); SA2.a (5′-GUACGGCAAUGUCAAUAUA-3′); and GFP Duplex I (Thermo Fisher Scientific).

Cell synchronization and siRNA transfection
Cells were synchronized essentially as described previously (McGuinness et al., 2005). In brief, HeLa1.2.11 cells were grown in the presence of 2 mM thymidine for 24 h, washed three times with PBS, and released into fresh medium for 4 h. Cells were then transfected with siRNA as described above. After 4 h, the medium was replaced with fresh medium and cells were further incubated for 4 h. 2 mM thymidine was then added and the cells were incubated for 12 h, washed three times with PBS, and released into fresh medium. Cells were then harvested by trypsinization at 2 and 4 h for FACS analysis and at 4 h for chromosome-specific FISH as described below.

FACS analysis
siRNA-transfected, trypsinized cells were washed twice with PBS containing 2 mM EDTA, fixed in cold 70% ethanol and stained with propidium iodide (50 μg/ml), and analyzed using a Becton Dickinson FACScan and FlowJo 8.8.6 software.

Immunoblot analysis
Whole cell extracts were prepared and immunoblots performed exactly as described previously (Canudas et al., 2007). siRNA-transfected HeLa1.2.11 cells were resuspended in four volumes of buffer C (20 mM Hepes-KOH, pH 7.9, 420 mM KCl, 25% glycerol, 0.1 mm EDTA, 5 mM $MgCl_2$, 0.2% NP40, 1 mM dithiothreitol [DTT], and 2.5% protease inhibitor cocktail [Sigma-Aldrich]) and incubated for 1 h on ice. Suspensions were pelleted at 8,000 *g* for 10 min. 25 μg (determined by Bio-Rad Laboratories protein assay) of supernatant proteins were fractionated by SDS-PAGE and analyzed by immunoblotting.

Immunoblots were incubated with the following primary antibodies: goat anti-SA1 BL143G (1 μg/ml, Bethyl Laboratories, Inc.); goat anti-SA2 BL146G (1 μg/ml, Bethyl Laboratories, Inc.); rabbit anti-Scc1 (2 mg/ml, Bethyl Laboratories, Inc.); rabbit anti-Smc3 (0.2 mg/ml, EMD); rabbit anti-TRF1 415 (1 μg/ml, Cook et al., 2002); rabbit anti-TIN2 701 (0.5 μg/ml, Houghtaling et al., 2004); and mouse anti-α–tubulin ascites (1:500,000; Sigma-Aldrich).

Chromosome-specific FISH
siRNA-transfected HeLa1.2.11 cells were collected by mitotic shake-off, fixed, and processed as described previously (Dynek and Smith, 2004). In brief, cells were fixed twice in methanol/acetic acid (3:1) for 15 min, cytospun (Shandon Cytospin) at 2,000 rpm for 2 min onto slides, rehydrated in 2X SSC at 37°C for 2 min, and dehydrated in an ethanol series of 70, 80, and 95% for 2 min each. Cells were denatured at 75°C for 2 min and hybridized overnight at 37°C with a subtelomeric FITC-conjugated probe (16pter, 4pter, or 20qter), a chromosome 6–specific alpha-satellite TRITC-conjugated centromere probe (6cen), a FITC-conjugated chromosome 10 centromere probe (10cen), or an arm Texas red–conjugated probe (JAG1 [20p12] or CUGBP2 [10p14]; Cytocell). Cells were washed in 0.4X SSC at 72°C for 2 min, and in 2X SSC with 0.05% Tween 20 at room temperature for 30 s. DNA was stained with 4,6-diamino-2-phenylindole (DAPI; 0.2 μg/ml). The distance between FISH signals was measured using OpenLab software (PerkinElmer).

Prometaphase spread analysis
For prometaphase spread analysis, siRNA-transfected HeLa1.2.11 cells were collected by trypsinization (0.5 mg/ml colcemide was added 60–90 min before harvest), swollen in hypotonic buffer containing 10 mM Tris-HCl, pH 7.4, 10 mM NaCl, and 5 mM $MgCl_2$ for 10 min at 37°C, and sedimented onto coverslips for 15 s at 1,000 rpm in a centrifuge (model RT7; Sorval). Cells were fixed with 2% paraformaldehyde and stained with rabbit anti-Smc2 (0.4 μg/ml; Bethyl Laboratories, Inc.). Primary antibodies were detected with FITC-conjugated donkey anti–rabbit antibodies (1:100; Jackson ImmunoResearch Laboratories, Inc.). DNA was stained with DAPI (0.2 μg/ml).

Chromosome-specific FISH of BrdU-positive cells
BrdU (10 μM) was added to siRNA-transfected HeLa1.2.11 cells for 1 h before harvest. Cells were collected by trypsinization, fixed twice in methanol/acetic acid (3:1) for 15 min, cytospun (Shandon Cytospin) at 2,000 rpm for 2 min onto slides, rehydrated in 2X SSC at 37°C for 2 min, and dehydrated in an ethanol series of 70, 80, and 95% for 2 min each. Samples were denatured in 70% Formamide/2X SSC at 72° for 2 min, dehydrated in 70, 90, 100% ethanol for 2 min each, and stained with mouse anti-BrdU (Becton Dickinson), followed by donkey anti–mouse TRITC. Samples were post-fixed in 3:1 methanol/acetic acid for 10 min, then in 2% paraformaldehyde for 1 min, and then dehydrated in 70, 90, 100% ethanol for 2 min each. Samples were then hybridized to the 16pter subtelomere FITC-conjugated probe and stained with DAPI (0.2 μg/ml).

PNA-FISH of prometaphase spreads
siRNA-transfected HeLa1.2.11 cells were collected by trypsinization (0.5 mg/ml colcemide was added 2 h before harvest), swollen in hypotonic

buffer for 10 min at 37°C, and fixed and processed exactly as described previously (Dynek and Smith, 2004). Chromosomes were hybridized to a Cy3-conjugated $(CCCTAA)_3$ telomere repeat probe (Applied Biosystems).

For ionizing radiation treatment, siRNA-transfected HeLaI.2.11 cells were irradiated with a ^{137}Cs source at a dose of 80 cGY/min and then incubated for 0 or 2 h before addition of colcemide. For the dose curve, cells were incubated for 2 h after radiation, processed as described above, and mitotic cells were scored by DAPI staining.

Image acquisition

Images were acquired using a microscope (Axioplan 2; Carl Zeiss, Inc.) with a Plan Apochrome 63x NA 1.4 oil immersion lens (Carl Zeiss, Inc.) and a digital camera (C4742-95; Hamamatsu Photonics). Images were acquired and processed using OpenLab software (PerkinElmer).

Online supplemental material

Fig. S1 shows immunoblot analysis of siRNA-treated HeLaI.2.11 cells. Fig. S2 A shows FISH analysis of siRNA-treated HeLaI.2.11 cells with telomere probe 4p. Fig. S2 B shows FISH analysis of TRF1 siRNA-treated HeLaI.2.11 cells with telomere probe 16p. Fig. S3 shows FACS analysis of synchronized siRNA-treated HeLaI.2.11 cells. Table S1 shows measurements of the average distance between paired FISH signals in siRNA-treated mitotic HeLaI.2.11 cells. Table S2 shows measurements of the average distance between chromosome arms in prometaphase spreads from siRNA-treated HeLaI.2.11 cells. Table S3 shows analysis of chromosomal morphology in HeLaI.2.11 double siRNA-treated prometaphase spreads. Table S4 shows analysis of mitotic index in GFP siRNA-treated cells after increasing dose of ionizing radiation. Table S5 shows analysis of mitotic index in GFP, TIN2, SA1, and SA2 siRNA-treated cells after 2 Gy ionizing radiation. Online supplemental material is available at http://www.jcb.org/cgi/content/full/jcb.200903096/DC1.

We thank Tom Meier and members of the Smith lab for comments on the manuscript and helpful discussion.

This work was supported by National Institutes of Health grant R01 CA116352.

Submitted: 17 March 2009
Accepted: 10 September 2009

References

Ancelin, K., M. Brunori, S. Bauwens, C.E. Koering, C. Brun, M. Ricoul, J.P. Pommier, L. Sabatier, and E. Gilson. 2002. Targeting assay to study the cis functions of human telomeric proteins: evidence for inhibition of telomerase by TRF1 and for activation of telomere degradation by TRF2. *Mol. Cell. Biol.* 22:3474–3487. doi:10.1128/MCB.22.10.3474-3487.2002

Anderson, D.E., A. Losada, H.P. Erickson, and T. Hirano. 2002. Condensin and cohesin display different arm conformations with characteristic hinge angles. *J. Cell Biol.* 156:419–424. doi:10.1083/jcb.200111002

Blasco, M.A. 2007. The epigenetic regulation of mammalian telomeres. *Nat. Rev. Genet.* 8:299–309. doi:10.1038/nrg2047

Canudas, S., B.R. Houghtaling, J.Y. Kim, J.N. Dynek, W.G. Chang, and S. Smith. 2007. Protein requirements for sister telomere association in human cells. *EMBO J.* 26:4867–4878. doi:10.1038/sj.emboj.7601903

Cesare, A.J., and R.R. Reddel. 2008. Telomere uncapping and alternative lengthening of telomeres. *Mech. Ageing Dev.* 129:99–108. doi:10.1016/j.mad.2007.11.006

Chang, C.R., C.S. Wu, Y. Hom, and M.R. Gartenberg. 2005. Targeting of cohesin by transcriptionally silent chromatin. *Genes Dev.* 19:3031–3042. doi:10.1101/gad.1356305

Cook, B.D., J.N. Dynek, W. Chang, G. Shostak, and S. Smith. 2002. Role for the related poly(ADP-Ribose) polymerases tankyrase 1 and 2 at human telomeres. *Mol. Cell. Biol.* 22:332–342. doi:10.1128/MCB.22.1.332-342.2002

de Lange, T. 2005. Shelterin: the protein complex that shapes and safeguards human telomeres. *Genes Dev.* 19:2100–2110. doi:10.1101/gad.1346005

Dynek, J.N., and S. Smith. 2004. Resolution of sister telomere association is required for progression through mitosis. *Science.* 304:97–100. doi:10.1126/science.1094754

Giménez-Abián, J.F., I. Sumara, T. Hirota, S. Hauf, D. Gerlich, C. de la Torre, J. Ellenberg, and J.M. Peters. 2004. Regulation of sister chromatid cohesion between chromosome arms. *Curr. Biol.* 14:1187–1193. doi:10.1016/j.cub.2004.06.052

Gruber, S., C.H. Haering, and K. Nasmyth. 2003. Chromosomal cohesin forms a ring. *Cell.* 112:765–777. doi:10.1016/S0092-8674(03)00162-4

Haering, C.H., J. Löwe, A. Hochwagen, and K. Nasmyth. 2002. Molecular architecture of SMC proteins and the yeast cohesin complex. *Mol. Cell.* 9:773–788. doi:10.1016/S1097-2765(02)00515-4

Houghtaling, B.R., L. Cuttonaro, W. Chang, and S. Smith. 2004. A dynamic molecular link between the telomere length regulator TRF1 and the chromosome end protector TRF2. *Curr. Biol.* 14:1621–1631. doi:10.1016/j.cub.2004.08.052

Hsiao, S.J., and S. Smith. 2009. Sister telomeres rendered dysfunctional by persistent cohesion are fused by NHEJ. *J. Cell Biol.* 184:515–526. doi:10.1083/jcb.200810132

Kim, S.H., P. Kaminker, and J. Campisi. 1999. TIN2, a new regulator of telomere length in human cells. *Nat. Genet.* 23:405–412 (see comments). doi:10.1038/70508

Losada, A., M. Hirano, and T. Hirano. 1998. Identification of *Xenopus* SMC protein complexes required for sister chromatid cohesion. *Genes Dev.* 12:1986–1997. doi:10.1101/gad.12.13.1986

Losada, A., T. Yokochi, R. Kobayashi, and T. Hirano. 2000. Identification and characterization of SA/Scc3p subunits in the *Xenopus* and human cohesin complexes. *J. Cell Biol.* 150:405–416. doi:10.1083/jcb.150.3.405

McGuinness, B.E., T. Hirota, N.R. Kudo, J.M. Peters, and K. Nasmyth. 2005. Shugoshin prevents dissociation of cohesin from centromeres during mitosis in vertebrate cells. *PLoS Biol.* 3:e86. doi:10.1371/journal.pbio.0030086

Michaelis, C., R. Ciosk, and K. Nasmyth. 1997. Cohesins: chromosomal proteins that prevent premature separation of sister chromatids. *Cell.* 91:35–45. doi:10.1016/S0092-8674(01)80007-6

Schmitz, J., E. Watrin, P. Lénárt, K. Mechtler, and J.M. Peters. 2007. Sororin is required for stable binding of cohesin to chromatin and for sister chromatid cohesion in interphase. *Curr. Biol.* 17:630–636. doi:10.1016/j.cub.2007.02.029

Sjögren, C., and K. Nasmyth. 2001. Sister chromatid cohesion is required for postreplicative double-strand break repair in *Saccharomyces cerevisiae*. *Curr. Biol.* 11:991–995. doi:10.1016/S0960-9822(01)00271-8

Smith, S., and T. de Lange. 2000. Tankyrase promotes telomere elongation in human cells. *Curr. Biol.* 10:1299–1302. doi:10.1016/S0960-9822(00)00752-1

Smith, S., I. Giriat, A. Schmitt, and T. de Lange. 1998. Tankyrase, a poly(ADP-ribose) polymerase at human telomeres. *Science.* 282:1484–1487 (see comments). doi:10.1126/science.282.5393.1484

Sumara, I., E. Vorlaufer, C. Gieffers, B.H. Peters, and J.M. Peters. 2000. Characterization of vertebrate cohesin complexes and their regulation in prophase. *J. Cell Biol.* 151:749–762. doi:10.1083/jcb.151.4.749

van Steensel, B., and T. de Lange. 1997. Control of telomere length by the human telomeric protein TRF1. *Nature.* 385:740–743. doi:10.1038/385740a0

van Steensel, B., A. Smogorzewska, and T. de Lange. 1998. TRF2 protects human telomeres from end-to-end fusions. *Cell.* 92:401–413. doi:10.1016/S0092-8674(00)80932-0

Waizenegger, I.C., S. Hauf, A. Meinke, and J.M. Peters. 2000. Two distinct pathways remove mammalian cohesin from chromosome arms in prophase and from centromeres in anaphase. *Cell.* 103:399–410. doi:10.1016/S0092-8674(00)00132-X

Zhang, N., S.G. Kuznetsov, S.K. Sharan, K. Li, P.H. Rao, and D. Pati. 2008. A handcuff model for the cohesin complex. *J. Cell Biol.* 183:1019–1031. doi:10.1083/jcb.200801157